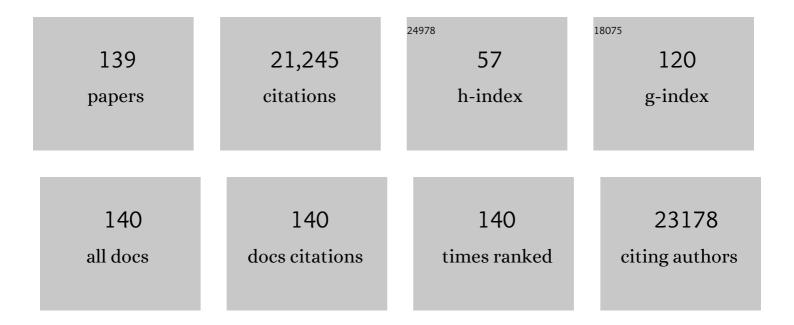
Tawfique Hasan

List of Publications by Year in descending order

Source: https://exaly.com/author-pdf/5387264/publications.pdf Version: 2024-02-01



| # | Article | IF | CITATIONS |
|----|---|------|-----------|
| 1 | Graphene photonics and optoelectronics. Nature Photonics, 2010, 4, 611-622. | 15.6 | 6,719 |
| 2 | Graphene Mode-Locked Ultrafast Laser. ACS Nano, 2010, 4, 803-810. | 7.3 | 1,795 |
| 3 | Inkjet-Printed Graphene Electronics. ACS Nano, 2012, 6, 2992-3006. | 7.3 | 1,018 |
| 4 | Production and processing of graphene and 2d crystals. Materials Today, 2012, 15, 564-589. | 8.3 | 866 |
| 5 | Nanotube–Polymer Composites for Ultrafast Photonics. Advanced Materials, 2009, 21, 3874-3899. | 11.1 | 778 |
| 6 | Functional inks and printing of two-dimensional materials. Chemical Society Reviews, 2018, 47, 3265-3300. | 18.7 | 401 |
| 7 | Sub 200 fs pulse generation from a graphene mode-locked fiber laser. Applied Physics Letters, 2010, 97, . | 1.5 | 398 |
| 8 | A stable, wideband tunable, near transform-limited, graphene-mode-locked, ultrafast laser. Nano Research, 2010, 3, 653-660. | 5.8 | 351 |
| 9 | Miniaturization of optical spectrometers. Science, 2021, 371, . | 6.0 | 321 |
| 10 | Black phosphorus ink formulation for inkjet printing of optoelectronics and photonics. Nature Communications, 2017, 8, 278. | 5.8 | 311 |
| 11 | Single-nanowire spectrometers. Science, 2019, 365, 1017-1020. | 6.0 | 291 |
| 12 | Tm-doped fiber laser mode-locked by graphene-polymer composite. Optics Express, 2012, 20, 25077. | 1.7 | 272 |
| 13 | Solution processed MoS2-PVA composite for sub-bandgap mode-locking of a wideband tunable ultrafast Er:fiber laser. Nano Research, 2015, 8, 1522-1534. | 5.8 | 256 |
| 14 | Oxygen self-doped g-C ₃ N ₄ with tunable electronic band structure for unprecedentedly enhanced photocatalytic performance. Nanoscale, 2018, 10, 4515-4522. | 2.8 | 247 |
| 15 | Printed gas sensors. Chemical Society Reviews, 2020, 49, 1756-1789. | 18.7 | 216 |
| 16 | Ultrafast lasers mode-locked by nanotubes and graphene. Physica E: Low-Dimensional Systems and Nanostructures, 2012, 44, 1082-1091. | 1.3 | 213 |
| 17 | A self-powered high-performance graphene/silicon ultraviolet photodetector with ultra-shallow junction: breaking the limit of silicon?. Npj 2D Materials and Applications, 2017, 1, . | 3.9 | 211 |
| 18 | Few-layer MoS_2 saturable absorbers for short-pulse laser technology: current status and future perspectives [Invited]. Photonics Research, 2015, 3, A30. | 3.4 | 185 |

| # | Article | IF | CITATIONS |
|----|--|------|-----------|
| 19 | Photoluminescence Spectroscopy of Carbon Nanotube Bundles: Evidence for Exciton Energy Transfer. Physical Review Letters, 2007, 99, 137402. | 2.9 | 181 |
| 20 | Ultra-strong nonlinear optical processes and trigonal warping in MoS2 layers. Nature Communications, 2017, 8, 893. | 5.8 | 177 |
| 21 | Bio-inspired Murray materials for mass transfer and activity. Nature Communications, 2017, 8, 14921. | 5.8 | 176 |
| 22 | Stabilization and "Debundling―of Single-Wall Carbon Nanotube Dispersions in <i>N</i> -Methyl-2-pyrrolidone (NMP) by Polyvinylpyrrolidone (PVP). Journal of Physical Chemistry C, 2007, 111, 12594-12602. | 1.5 | 158 |
| 23 | Fast Response and High Sensitivity ZnO/glass Surface Acoustic Wave Humidity Sensors Using Graphene Oxide Sensing Layer. Scientific Reports, 2014, 4, 7206. | 1.6 | 149 |
| 24 | Carbon Nanotube Polycarbonate Composites for Ultrafast Lasers. Advanced Materials, 2008, 20, 4040-4043. | 11.1 | 148 |
| 25 | Ab initio study of electronic and optical behavior of two-dimensional silicon carbide. Journal of Materials Chemistry C, 2013, 1, 2131. | 2.7 | 148 |
| 26 | Sensitive Electronic-Skin Strain Sensor Array Based on the Patterned Two-Dimensional α-ln ₂ Se ₃ . Chemistry of Materials, 2016, 28, 4278-4283. | 3.2 | 146 |
| 27 | Density Gradient Ultracentrifugation of Nanotubes: Interplay of Bundling and Surfactants Encapsulation. Journal of Physical Chemistry C, 2010, 114, 17267-17285. | 1.5 | 144 |
| 28 | Optical Waveplates Based on Birefringence of Anisotropic Two-Dimensional Layered Materials. ACS Photonics, 2017, 4, 3023-3030. | 3.2 | 144 |
| 29 | Inkjet Printed Largeâ€Area Flexible Few‣ayer Graphene Thermoelectrics. Advanced Functional Materials, 2018, 28, 1800480. | 7.8 | 136 |
| 30 | Engineering symmetry breaking in 2D layered materials. Nature Reviews Physics, 2021, 3, 193-206. | 11.9 | 135 |
| 31 | Ultrafast stretched-pulse fiber laser mode-locked by carbon nanotubes. Nano Research, 2010, 3, 404-411. | 5.8 | 133 |
| 32 | Slow Photons for Photocatalysis and Photovoltaics. Advanced Materials, 2017, 29, 1605349. | 11.1 | 129 |
| 33 | Printed aerogels: chemistry, processing, and applications. Chemical Society Reviews, 2021, 50, 3842-3888. | 18.7 | 128 |
| 34 | A Fully Printed Flexible MoS ₂ Memristive Artificial Synapse with Femtojoule Switching Energy. Advanced Electronic Materials, 2019, 5, 1900740. | 2.6 | 123 |
| 35 | 74-fs nanotube-mode-locked fiber laser. Applied Physics Letters, 2012, 101, 153107. | 1.5 | 122 |
| 36 | Anisotropic Growth of Nonlayered CdS on MoS ₂ Monolayer for Functional Vertical Heterostructures, Advanced Functional Materials, 2016, 26, 2648-2654 | 7.8 | 118 |

| # | Article | IF | CITATIONS |
|----|--|------|-----------|
| 37 | Vertically aligned two-dimensional SnS ₂ nanosheets with a strong photon capturing capability for efficient photoelectrochemical water splitting. Journal of Materials Chemistry A, 2017, 5, 1989-1995. | 5.2 | 117 |
| 38 | 3D interconnected macro-mesoporous electrode with self-assembled NiO nanodots for high-performance supercapacitor-like Li-ion battery. Nano Energy, 2016, 22, 269-277. | 8.2 | 115 |
| 39 | 3D Ferroconcreteâ€Like Aminated Carbon Nanotubes Network Anchoring Sulfur for Advanced Lithium–Sulfur Battery. Advanced Energy Materials, 2018, 8, 1801066. | 10.2 | 115 |
| 40 | A compact, high power, ultrafast laser mode-locked by carbon nanotubes. Applied Physics Letters, 2009, 95, . | 1.5 | 114 |
| 41 | Manganese dioxide nanosheet functionalized sulfur@PEDOT core–shell nanospheres for advanced lithium–sulfur batteries. Journal of Materials Chemistry A, 2016, 4, 9403-9412. | 5.2 | 112 |
| 42 | 15 GHz picosecond pulse generation from a monolithic waveguide laser with a graphene-film saturable output coupler. Optics Express, 2013, 21, 7943. | 1.7 | 111 |
| 43 | A Broadband Fluorographene Photodetector. Advanced Materials, 2017, 29, 1700463. | 11.1 | 110 |
| 44 | 102 fs pulse generation from a long-term stable, inkjet-printed black phosphorus-mode-locked fiber laser. Optics Express, 2018, 26, 12506. | 1.7 | 104 |
| 45 | Inkjet-printed graphene electrodes for dye-sensitized solar cells. Carbon, 2016, 105, 33-41. | 5.4 | 94 |
| 46 | Anchoring ultrafine metallic and oxidized Pt nanoclusters on yolk-shell TiO2 for unprecedentedly high photocatalytic hydrogen production. Nano Energy, 2017, 38, 118-126. | 8.2 | 91 |
| 47 | A general ink formulation of 2D crystals for wafer-scale inkjet printing. Science Advances, 2020, 6, eaba5029. | 4.7 | 89 |
| 48 | 152 fs nanotube-mode-locked thulium-doped all-fiber laser. Scientific Reports, 2016, 6, 28885. | 1.6 | 86 |
| 49 | Broadly Defining Lasing Wavelengths in Single Bandgap-Graded Semiconductor Nanowires. Nano Letters, 2014, 14, 3153-3159. | 4.5 | 84 |
| 50 | Mid-infrared Raman-soliton continuum pumped by a nanotube-mode-locked sub-picosecond Tm-doped MOPFA. Optics Express, 2013, 21, 23261. | 1.7 | 74 |
| 51 | Lattice Dynamics, Phonon Chirality, and Spin–Phonon Coupling in 2D Itinerant Ferromagnet Fe ₃ GeTe ₂ . Advanced Functional Materials, 2019, 29, 1904734. | 7.8 | 70 |
| 52 | Graphene charge-injection photodetectors. Nature Electronics, 2022, 5, 281-288. | 13.1 | 70 |
| 53 | Hierarchy Design in Metal Oxides as Anodes for Advanced Lithiumâ€ion Batteries. Small Methods, 2018, 2, 1800171. | 4.6 | 69 |
| 54 | Double-Wall Carbon Nanotubes for Wide-Band, Ultrafast Pulse Generation. ACS Nano, 2014, 8, 4836-4847. | 7.3 | 66 |

| # | Article | IF | CITATIONS |
|----|--|-----|-----------|
| 55 | Hierarchical Zeolite Single-Crystal Reactor for Excellent Catalytic Efficiency. Matter, 2020, 3, 1226-1245. | 5.0 | 66 |
| 56 | Hydrophilic bi-functional B-doped g-C3N4 hierarchical architecture for excellent photocatalytic H2O2 production and photoelectrochemical water splitting. Journal of Energy Chemistry, 2022, 70, 236-247. | 7.1 | 66 |
| 57 | Selenium clusters in Zn-glutamate MOF derived nitrogen-doped hierarchically radial-structured microporous carbon for advanced rechargeable Na–Se batteries. Journal of Materials Chemistry A, 2018, 6, 22790-22797. | 5.2 | 62 |
| 58 | Ultrafast Raman laser mode-locked by nanotubes. Optics Letters, 2011, 36, 3996. | 1.7 | 60 |
| 59 | Double-Wall Carbon Nanotube Hybrid Mode-Locker in Tm-doped Fibre Laser: A Novel Mechanism for Robust Bound-State Solitons Generation. Scientific Reports, 2017, 7, 44314. | 1.6 | 57 |
| 60 | Wavelength and pulse duration tunable ultrafast fiber laser mode-locked with carbon nanotubes. Scientific Reports, 2018, 8, 2738. | 1.6 | 57 |
| 61 | Designing an Efficient Multimode Environmental Sensor Based on Graphene–Silicon Heterojunction. Advanced Materials Technologies, 2017, 2, 1600262. | 3.0 | 55 |
| 62 | Q-switched Dy:ZBLAN fiber lasers beyond 3 14 m: comparison of pulse generation using acousto-optic modulation and inkjet-printed black phosphorus. Optics Express, 2019, 27, 15032. | 1.7 | 54 |
| 63 | 320 fs pulse generation from an ultrafast laser inscribed waveguide laser mode-locked by a nanotube saturable absorber. Applied Physics Letters, 2010, 97, 111114. | 1.5 | 53 |
| 64 | Unique walnut-shaped porous MnO ₂ /C nanospheres with enhanced reaction kinetics for lithium storage with high capacity and superior rate capability. Journal of Materials Chemistry A, 2016, 4, 4264-4272. | 5.2 | 53 |
| 65 | Solventâ€Based Softâ€Patterning of Graphene Lateral Heterostructures for Broadband Highâ€Speed Metal–Semiconductor–Metal Photodetectors. Advanced Materials Technologies, 2017, 2, 1600241. | 3.0 | 53 |
| 66 | Hierarchical nanosheet-constructed yolk–shell TiO ₂ porous microspheres for lithium batteries with high capacity, superior rate and long cycle capability. Nanoscale, 2015, 7, 12979-12989. | 2.8 | 51 |
| 67 | Characterization of carbon nanotube–thermotropic nematic liquid crystal composites. Journal Physics D: Applied Physics, 2008, 41, 125106. | 1.3 | 50 |
| 68 | Realization of vertical metal semiconductor heterostructures via solution phase epitaxy. Nature Communications, 2018, 9, 3611. | 5.8 | 49 |
| 69 | Three-Dimensional (3D) Bicontinuous Hierarchically Porous Mn2O3 Single Crystals for High Performance Lithium-Ion Batteries. Scientific Reports, 2015, 5, 14686. | 1.6 | 47 |
| 70 | Pulse dynamics in carbon nanotube mode-locked fiber lasers near zero cavity dispersion. Optics Express, 2015, 23, 9947. | 1.7 | 46 |
| 71 | Unprecedented and highly stable lithium storage capacity of (001) faceted nanosheet-constructed hierarchically porous TiO2/rGO hybrid architecture for high-performance Li-ion batteries. National Science Review, 2020, 7, 1046-1058. | 4.6 | 46 |
| 72 | Polymer-Assisted Isolation of Single Wall Carbon Nanotubes in Organic Solvents for Optical-Quality Nanotubeâ îPolymer Composites. Journal of Physical Chemistry C, 2008, 112, 20227-20232. | 1.5 | 45 |

| # | Article | IF | CITATIONS |
|----|--|-----|-----------|
| 73 | Synthesis of YBa ₂ Cu ₃ O _{7â^î^} and Y ₂ BaCuO ₅ Nanocrystalline Powders for YBCO Superconductors Using Carbon Nanotube Templates. ACS Nano, 2012, 6, 5395-5403. | 7.3 | 43 |
| 74 | Optimizing inner voids in yolk-shell TiO2 nanostructure for high-performance and ultralong-life lithium-sulfur batteries. Chemical Engineering Journal, 2021, 417, 129241. | 6.6 | 42 |
| 75 | Conformal Printing of Graphene for Single―and Multilayered Devices onto Arbitrarily Shaped 3D Surfaces. Advanced Functional Materials, 2019, 29, 1807933. | 7.8 | 40 |
| 76 | Ab initio optical study of graphene on hexagonal boron nitride and fluorographene substrates. Journal of Materials Chemistry C, 2013, 1, 1618. | 2.7 | 39 |
| 77 | Ultrafast nonlinear photoresponse of single-wall carbon nanotubes: a broadband degenerate investigation. Nanoscale, 2016, 8, 9304-9309. | 2.8 | 39 |
| 78 | Hierarchical TiO ₂ /C nanocomposite monoliths with a robust scaffolding architecture, mesopore–macropore network and TiO ₂ –C heterostructure for high-performance lithium ion batteries. Nanoscale, 2016, 8, 10928-10937. | 2.8 | 38 |
| 79 | Inkjetâ€Printed rGO/binary Metal Oxide Sensor for Predictive Gas Sensing in a Mixed Environment. Advanced Functional Materials, 2022, 32, . | 7.8 | 38 |
| 80 | Enhancing monolayer photoluminescence on optical micro/nanofibers for low-threshold lasing. Science Advances, 2019, 5, eaax7398. | 4.7 | 36 |
| 81 | Stable, Surfactant-Free Graphene-Styrene Methylmethacrylate Composite for Ultrafast Lasers. Advanced Optical Materials, 2016, 4, 1088-1097. | 3.6 | 35 |
| 82 | Theory of edge-state optical absorption in two-dimensional transition metal dichalcogenide flakes. Physical Review B, 2016, 94, . | 1.1 | 35 |
| 83 | Graphene actively Q-switched lasers. 2D Materials, 2017, 4, 025095. | 2.0 | 34 |
| 84 | Optical properties of nanotube bundles by photoluminescence excitation and absorption spectroscopy. Physica E: Low-Dimensional Systems and Nanostructures, 2008, 40, 2352-2359. | 1.3 | 33 |
| 85 | 500fs wideband tunable fiber laser mode-locked by nanotubes. Physica E: Low-Dimensional Systems and Nanostructures, 2012, 44, 1078-1081. | 1.3 | 33 |
| 86 | High-energy and efficient Raman soliton generation tunable from 198 to 229  µm in an all-silica-fiber thulium laser system. Optics Letters, 2017, 42, 3518. | 1.7 | 31 |
| 87 | Nanotubes Complexed with DNA and Proteins for Resistive-Pulse Sensing. ACS Nano, 2013, 7, 8857-8869. | 7.3 | 30 |
| 88 | Inkjet-printed CMOS-integrated graphene–metal oxide sensors for breath analysis. Npj 2D Materials and Applications, 2019, 3, . | 3.9 | 30 |
| 89 | Surfactantâ€∎ided exfoliation of molybdenum disulfide for ultrafast pulse generation through edgeâ€state saturable absorption. Physica Status Solidi (B): Basic Research, 2016, 253, 911-917. | 0.7 | 29 |
| 90 | Flexible Dielectric Nanocomposites with Ultrawide Zero-Temperature Coefficient Windows for Electrical Energy Storage and Conversion under Extreme Conditions. ACS Applied Materials & Interfaces, 2017, 9, 7591-7600. | 4.0 | 29 |

| # | Article | IF | CITATIONS |
|-----|---|-------------------|--------------------|
| 91 | Hexagonal Boron Nitride–Enhanced Optically Transparent Polymer Dielectric Inks for Printable Electronics. Advanced Functional Materials, 2020, 30, 2002339. | 7.8 | 29 |
| 92 | Functional inks of graphene, metal dichalcogenides and black phosphorus for photonics and (opto)electronics. Proceedings of SPIE, 2015, , . | 0.8 | 27 |
| 93 | Wavelength tunable soliton rains in a nanotube-mode locked Tm-doped fiber laser. Applied Physics Letters, 2018, 113, . | 1.5 | 26 |
| 94 | Printing of Graphene and Related 2D Materials. , 2019, , . | | 25 |
| 95 | Interwoven scaffolded porous titanium oxide nanocubes/carbon nanotubes framework for high-performance sodium-ion battery. Journal of Energy Chemistry, 2021, 59, 38-46. | 7.1 | 25 |
| 96 | Scalar Nanosecond Pulse Generation in a Nanotube Mode-Locked Environmentally Stable Fiber Laser. IEEE Photonics Technology Letters, 2014, 26, 1672-1675. | 1.3 | 24 |
| 97 | Hysteresis suppression in self-assembled single-wall nanotube field effect transistors. Physica E: Low-Dimensional Systems and Nanostructures, 2008, 40, 2278-2282. | 1.3 | 23 |
| 98 | Single-cell yolk-shell nanoencapsulation for long-term viability with size-dependent permeability and molecular recognition. National Science Review, 2021, 8, nwaa097. | 4.6 | 23 |
| 99 | Environmentally stable black phosphorus saturable absorber for ultrafast laser. Nanophotonics, 2020, 9, 2445-2449. | 2.9 | 21 |
| 100 | 172  fs, 243  kW peak power pulse generation from a Ho-doped fiber laser system. Optics Let 4619. | ters, 2018 1.7 | , 43 ₂₀ |
| 101 | Machine-intelligent inkjet-printed α-Fe2O3/rGO towards NO2 quantification in ambient humidity. Sensors and Actuators B: Chemical, 2020, 321, 128446. | 4.0 | 20 |
| 102 | Dispersibility and stability improvement of unfunctionalized nanotubes in amide solvents by polymer wrapping. Physica E: Low-Dimensional Systems and Nanostructures, 2008, 40, 2414-2418. | 1.3 | 19 |
| 103 | Q-switched Fiber Laser with MoS2 Saturable Absorber. , 2014, , . | | 19 |
| 104 | 3D interconnected hierarchically macro-mesoporous TiO ₂ networks optimized by biomolecular self-assembly for high performance lithium ion batteries. RSC Advances, 2016, 6, 26856-26862. | 1.7 | 19 |
| 105 | Evanescent-wave coupled right angled buried waveguide: Applications in carbon nanotube mode-locking. Applied Physics Letters, 2013, 103, 221117. | 1.5 | 18 |
| 106 | Broad bandwidth dual-wavelength fiber laser simultaneously delivering stretched pulse and dissipative soliton. Optics Express, 2020, 28, 6937. | 1.7 | 17 |
| 107 | Unprecedented strong and reversible atomic orbital hybridization enables a highly stable Li–S battery. National Science Review, 2022, 9, . | 4.6 | 15 |
| 108 | Spectroscopic characterization of protein-wrapped single-wall carbon nanotubes and quantification of their cellular uptake in multiple cell generations. Nanotechnology, 2013, 24, 265102. | 1.3 | 14 |

1

| # | Article | IF | CITATIONS |
|-----|---|-------------|-----------|
| 109 | Vertically aligned smooth ZnO nanorod films for planar device applications. Journal of Materials Chemistry C, 2013, 1, 2525. | 2.7 | 13 |
| 110 | Sub-150 fs dispersion-managed soliton generation from an all-fiber Tm-doped laser with BP-SA. Optics Express, 2020, 28, 34104. | 1.7 | 12 |
| 111 | Fiber-Integrated Reversibly Wavelength-Tunable Nanowire Laser Based on Nanocavity Mode Coupling. ACS Nano, 2019, 13, 9965-9972. | 7.3 | 11 |
| 112 | Giant All-Optical Modulation of Second-Harmonic Generation Mediated by Dark Excitons. ACS Photonics, 2021, 8, 2320-2328. | 3.2 | 11 |
| 113 | All-Fiber Passively Q-Switched Laser Based on Tm3+-Doped Tellurite Fiber. IEEE Photonics Technology Letters, 2015, 27, 689-692. | 1.3 | 10 |
| 114 | New Approach for Thickness Determination of Solution-Deposited Graphene Thin Films. ACS Omega, 2017, 2, 2630-2638. | 1.6 | 8 |
| 115 | Thickness modulations enable multi-functional spin valves based on Van der Waals hetero-structure. Nano Today, 2022, 42, 101373. | 6.2 | 8 |
| 116 | Coexistence of Contact Electrification and Dynamic p–n Junction Modulation Effects in Triboelectrification. ACS Applied Materials & Interfaces, 2022, 14, 30410-30419. | 4.0 | 8 |
| 117 | Soliton Mode-Locked Large-Mode-Area Tm-Doped Fiber Oscillator. IEEE Photonics Technology Letters, 2020, 32, 117-120. | 1.3 | 7 |
| 118 | 100 m min ^{â^'1} Industrial‣cale Flexographic Printing of Grapheneâ€Incorporated Conduc Ink. Advanced Engineering Materials, 2022, 24, 2101217. | tive 1.6 | 7 |
| 119 | Controlling surface porosity of graphene-based printed aerogels. Npj 2D Materials and Applications, 2022, 6, . | 3.9 | 6 |
| 120 | Fluorinated graphene and hexagonal boron nitride as ALD seed layers for graphene-based van der Waals heterostructures. Nanotechnology, 2014, 25, 355202. | 1.3 | 5 |
| 121 | High-Power Femtosecond Pulse Generation From an All-Fiber Er-Doped Chirped Pulse Amplification System. IEEE Photonics Journal, 2020, 12, 1-8. | 1.0 | 3 |
| 122 | Structures, Properties and Applications of 2D Materials. , 2019, , 19-51. | | 2 |
| 123 | 2D Material Production Methods. , 2019, , 53-101. | | 2 |
| 124 | Printing Technologies. , 2019, , 135-178. | | 2 |
| 125 | 2D Ink Design. , 2019, , 103-134. | | 2 |
| | | | |

126 Ultrafast nonlinear absorption in SWNTs: An ultra-broadband investigation. , 2015, , .

| # | Article | IF | CITATIONS |
|-----|--|------|-----------|
| 127 | Photodetectors: A Broadband Fluorographene Photodetector (Adv. Mater. 22/2017). Advanced Materials, 2017, 29, . | 11.1 | 1 |
| 128 | Applications of Printed 2D Materials. , 2019, , 179-216. | | 1 |
| 129 | Nanotube mode-locked, low repetition rate pulse source for fiber-based supercontinuum generation at low average pump power. , 2014, , . | | 1 |
| 130 | Fabrication and mechanical property of carbon nanotube/metal composites. , 2010, , . | | 0 |
| 131 | Q-switched modelocking using carbon nanotubes in an ultrafast laser inscribed ytterbium doped bismuthate glass waveguide laser. , 2012, , . | | 0 |
| 132 | Spectroscopic characteristics and cellular compatibility of protein wrapped single wall carbon nanotubes. , 2012, , . | | 0 |
| 133 | Improving the efficiency of nanowire based ultraviolet light emitting diode. , 2015, , . | | 0 |
| 134 | Wideband tunable ultrafast fiber laser using blackphosphorus saturable absorber. , 2017, , . | | 0 |
| 135 | Observation of tunable dual-wavelength in a fiber laser mode-locked by black phosphorus. , 2017, , . | | 0 |
| 136 | Manufacturing 2D Material Based Saturable Absorbers: From Composites to Printing. , 2021, , . | | 0 |
| 137 | Q-switched pulse generation in Yb- and Er-doped fiber laser with WS2 saturable absorber. , 2015, , . | | 0 |
| 138 | 136fs, 6 nJ thulium-based all-fiber CPA system. , 2016, , . | | 0 |
| 139 | Graphene-based inkjet-printable electrodes for dye-sensitized solar cells. Acta Crystallographica Section A: Foundations and Advances, 2017, 73, C1070-C1070. | 0.0 | ο |